Multimedia Tools and Applications (2023) 82:16555–16589
https://doi.org/10.1007/s11042-022-14002-8

Robust, imperceptible and optimized watermarking of DICOM image using Schur decomposition, LWT-DCT-SVD and its authentication using SURF

Divyanshu Awasthi [1] · Vinay Kumar Srivastava [1]

Received: 24 May 2022 / Revised: 21 July 2022 / Accepted: 19 September 2022 /
Published online: 27 September 2022

Abstract
In this proposed work, a dual image watermarking algorithm is used to protect the data against copyright violations. In this work, the DICOM image is used as a host image. Two watermark images used are the MNNIT logo and the personal data of the patient. This method utilizes the advantages of Schur decomposition, lifting wavelet transform (LWT), discrete cosine transform (DCT) and singular value decomposition (SVD). The scaling factor is a vital parameter of watermarking technique. The firefly optimization technique is used to get the optimized scaling factor. The Speeded-up robust features (SURF) are used for watermarking authentication. To evaluate the performance of the proposed algorithm, peak signal-to-noise ratio (PSNR), normalized correlation coefficient (NCC), and structural similarity index measurement (SSIM) are used. The proposed method is tested against various attacks such as Salt and Pepper noise, Gaussian noise, Gaussian low pass filter, Average filter, Median filter, Histogram equalization, Sharpening, Rotation and Region of interest filtering. The proposed algorithm shows a high level of robustness and imperceptibility. It is found that the features of the input host image and the watermarked image are matching correctly on applying the SURF technique.

Keywords Schur decomposition · Lifting wavelet transform (LWT) · Discrete cosine transform (DCT) · Singular value decomposition (SVD) · Firefly optimization · SURF

✉ Divyanshu Awasthi
divyanshuawasthi83@gmail.com

Vinay Kumar Srivastava
Vinay@mnnit.ac.in

[1] Electronics & Communication Engineering Department, Motilal Nehru National Institute of Technology, Prayagraj, Uttar Pradesh 211004, India

1 Introduction

With the rapid development of digital technologies, several pressing security concerns have arisen, including the unlawful copying and distortion of private information. Digital image watermarking is thought to be a viable solution to these security concerns. In a watermarking algorithm, invisibility denotes the cover image and the watermarked image being similar enough to avoid being spotted. The robustness of the watermark shows that the watermark algorithm can withstand frequent attacks. DICOM stands for Digital Imaging and Communications in Medicine and it is a global standard for storing, exchanging and transmitting medical pictures. This standard is used by image technologies such as X-rays, ultrasound, microscopy, MRI and CT. The standard provides several benefits, including: (1) Both image and patient information will be transferred in a single network session, (2) Patient safety is improved, and (3) Save detailed acquisition and diagnostic protocol information. The recent literature survey of image watermarking methods is listed in Table 1.

From the literature survey presented in Table 1, it can be summarized that image watermarking poses several possible risks and challenges. Finding a balance between imperceptibility, resilience, and capacity is the first challenge because enhancing one aspect has a detrimental impact on the others. An effective watermarking system should have all three traits at once. The amount of data conveyed is referred to as the payload size. Less imperceptibility results from a larger payload. All of these features must be balanced out in a decent watermarking strategy. So, in this work, a method is proposed to get a highly robust and imperceptible dual image watermarking. The scaling factor plays a vital role in the proposed scheme, so to get the optimum value of the scaling factor, an optimization technique is used by taking a unique equation. Authentication is the process by which one can understand that the features of the watermarked medical image are valid and there is no adverse effect due to various attacks after applying the proposed watermarking scheme. In this work, SURF features are used for authentication purpose.

This paper is divided into the following sections: section 2 is related to the preliminaries, section 3 shows the proposed watermarking embedding and extraction process, section 4 is results and discussion, section 5 is related to the SURF feature authentication, and section 6 is the conclusion.

2 Preliminaries

The proposed watermarking technique uses LWT-DCT-SVD and Schur decomposition for embedding. The work proposed in this paper is different from [27], as in this work, Firefly optimization is used instead of Particle swarm optimization and the scheme is also a dual watermarking scheme. DWT-DCT-SVD with backpropagation neural network is used in [36] to get the watermarked image, but the proposed work uses LWT-DCT-SVD with Schur decomposition for embedding.

2.1 Lifting wavelet transform (LWT)

Sweldens [30] introduced the lifting wavelet transform in 1998. The lifting Wavelet reduces the challenge of reversibility by immediately examining the problem in the integer domain, which is not observed in standard Wavelet transforms. The advantages of LWT over typical

Table 1 Summary of the recent literature survey of image watermarking techniques

Ref. No.	Purpose	Techniques used	Input image	Performance parameters	Attacks	Remark
[1]	To propose a robust method for linear and non-linear attacks and the transparency of the watermarked images will be protected.	Discrete cosine transform (DCT), Discrete wavelet transform (DWT), Arnold transform (AT)	RGB host images: Baboon, Pears, Pepper, Jet plane, Barbara (1024x1024-x3); Watermark images: 96×96 grayscale Lena, Cameraman, and Saturn	Peak signal to noise ratio (PSNR), Normalized correlation coefficient (NCC)	Blurring, Average filter, Sharpening, Resizing, JPEG, Median filter, Salt and Pepper, Speckle, Rotation	By embedding the DCT transformed watermark parts separately into all the DWT bands of each color component of the cover image, high robustness and imperceptibility have been obtained with the proposed method.
[2]	Blind watermarking targets the recovery of the watermark when the host is not available during the detection stage	Discrete Shearlet Transform (DST), Discrete Wavelet Transform (DWT), Contourlet Transform (CT), Laplacian distribution	Host images of size 512×512: Baboon, Barbara, Clock, Cameraman, Pepper, Boat	Peak signal to noise ratio (PSNR), Structural similarity index measurement (SSIM), Root mean square error (RMSE)	–	The DST-based embedding provides a good imperceptibility and an improved payload, and the results demonstrate superior robustness against common image processing manipulations compared to DWT and CT
[3]	To get high robustness against noise addition attacks	Discrete cosine transform (DCT), Discrete wavelet transform (DWT), Arnold cat map	Host image of size 512×512: Barbara, Baboon, Pepper; Watermark logo: 32×32 binary image	Mean absolute error (MAE), Peak Signal to noise ratio (PSNR)	Salt and pepper noises, Cropping, JPEG compression, Gaussian low pass filter, Scaling	The proposed method has high imperceptibility and robustness against different types of attacks.
[4] [5]	This paper proposed a survey on watermarking methods in the artificial intelligence domain and beyond.					

Table 1 (continued)

Ref. No.	Purpose	Techniques used	Input image	Performance parameters	Attacks	Remark
	Dual Watermarking for Security of COVID-19 Patient Record.	Redundant discrete wavelet transform (RDWT), Hessenberg Decomposition (HD), Randomized singular value decomposition (RSVD)	Host image of size 512×512: CT scan images of COVID-19 patients Electronic patient record (266 bits) and watermark image (256×256)	Peak Signal to noise ratio (PSNR), Normalized correlation coefficient (NCC), Bit error rate (BER), Unified Average Change Intensity (UACI), Number of Pixels Change Rate (NPCR)	Salt and pepper noises, Gaussian noise, Rotation, JPEG compression, Speckle noise, Median filter, Cropping, Scaling, Translation	Imperceptibility and robustness are achieved by a fuzzy inference system. The extracted watermark is denoised using the concept of deep neural network (DNN) to improve its robustness.
[6]	To get significant improvement in transparency and the robustness under attacks.	Singular value decomposition (SVD), Genetic algorithm (GA)	Host image of size 256×256: Lena; Watermark image of size: 32×32 (grey-level)	Correlation coefficient (CC), PSNR	Rotation, Average filter, Scaling, Gaussian noise, Gamma correction, Histogram, Median filter	In the proposed method, GA is utilized to obtain multiple scaling factors (SF) for achieving the highest possible robustness without degrading image quality.
[7]	This paper provides a comparison between PSO and JAYA as well as between LWT and DWT	LWT, DWT, DCT, SVD, PSO, JAYA	Host grayscale image: 512×512; Watermark grayscale: 256×256	PSNR, SSIM, Normalized correlation coefficient (NCC), Mean square error (MSE)	JPEG compression, Gaussian noise, Median filter, Salt and Pepper, Low pass filter, Sharpening, Gamma correction, Scaling, Translation	The proposed work has been tested under different attacks and found robust and imperceptible.
[8]	To improve the watermarked image's integrity and perceived quality and to enhance the security of watermarking	DWT, SVD, Quantization,	Shore, Lena, Baboon, Pepper, Dark cloud: 200×200	PSNR, Bit error rate (BER)	JPEG compression, Gaussian noise, Median filter, Cropping	The enhanced perceptual quality of the watermarked images and the proposed scheme preserve high PSNR.
[10]	The proposed method uses 2-D Linear Discriminant Analysis	2-D linear discriminant analysis (2DLDA),	Host image: e 512×512, where	PSNR, Bit error rate (BER)	Cropping, Blurring, Mosaic, Luminance	Experimental results demonstrate that the

Table 1 (continued)

Ref. No.	Purpose	Techniques used	Input image	Performance parameters	Attacks	Remark
	(2DLDA) watermark scheme for copyright protection	Discrete cosine transform (DCT)	each pixel is represented by 24 bits in the RGB color space; watermark of a recognizable pattern of size 32×25		and contrast adjustment, JPEG	differences between the watermarked and original images are indistinguishable. The proposed method effectively resists standard image processing attacks.
[12]	This paper proposed a dual watermarking-based multi-media content authentication and privacy preservation so-lution.	DWT, DCT, Encryption, Arnold transform	Host grayscale image: 512× 512 Watermark grayscale: 64× 64	PSNR, BER (Bit error rate), NCC, BCR (Bit correction ratio)	JPEG, Gaussian noise, Salt and Pepper, Median filter, Gaussian LPF, Rotation, Brightness, Darkening, Scaling recovery, Wiener	A highly robust watermarking framework for copyright protection applications is proposed. It also serves the purpose of authentication.
[13]	This paper presents a reliable digital watermarking technique that provides high imperceptibility and robustness for copyright protection	Optimal discrete cosine transform (DCT), psychovisual threshold, Arnold transform	Host image of size 512×512: LENA, Baboon, Cameraman, Pepper, Airplane, Livingroom; Watermark image: a binary logo image with 32× 32 pixels	PSNR, BER (Bit error rate), NCC, Structural similarity index measurement (SSIM)	Sharpening, Histogram, JPEG, Average, Wiener, Median, GLP, Gaussian noise, Salt and Pepper, Adjust, JPEG2000	The proposed method has higher values of NC and SSIM when compared with other methods
[14]	In this paper, a robust and blind digital	DWT, DCT, SVD	Host grayscale image: 512× 512	PSNR, NCC, MSE (Mean square error)	Motion blur, Gaussian blur, Sharpening, Gaussian noise, Salt	The suggested approach has been resistant to most attacks, which can be verified by

Table 1 (continued)

Ref. No.	Purpose	Techniques used	Input image	Performance parameters	Attacks	Remark
	image watermarking technique is proposed to achieve copyright protection.		Watermark grayscale: 256 ×256		and Pepper, Contrast, Rotation, Crop, Negative, Swirl	recovering the watermark from any sub-bands.
[9]	The proposed method is used for copyright protection and authentication.	DWT, SVD, Zig-Zag sequence	Host grayscale image: 512× 512 Watermark grayscale: 128 ×128	PSNR, NCC	JPEG, JPEG2000, Gaussian noise, Resize, Rotation, Crop	The proposed Dual image watermarking is robust.
[15]	This paper proposed a dual watermarking-based multi-media content authentication and privacy preservation so-lution.	DWT, DCT, Encryption, Arnold transform	Host grayscale image: 512× 512 Watermark grayscale: 64× 64	PSNR, BER (Bit error rate), NCC, BCR (Bit correction ratio)	JPEG, Gaussian noise, Salt and Pepper, Median filter, Gaussian LPF, Rotation, Brightness, Darkening, Scaling recovery, Wiener filter,	A highly robust watermarking framework for copyright protection applications is proposed. It also serves the purpose of authentication.
[16]	To provide both robustness and imperceptibility	DWT, SVD	Host grayscale image: 512× 512; Watermark grayscale: 256 ×256	Peak signal to noise ratio (PSNR), Normalized correlation coefficient (NCC)	Gaussian blurring, Histogram eq., Rotation, JPEG, Salt & Pepper, Gamma correction, Median filtering	Significant improvement in imperceptibility and robustness under various attacks
[17]	To optimize the tradeoff between imperceptibility and robustness properties, this paper proposes a robust and invisible blind image watermarking scheme	DWT, DCT, SVD, Chaotic map	Host image size of 512×512: Boat, Lena, Livingroom, Mandrill, Peppers, Pirate, Jet plane, Lake;	Peak signal to noise ratio (PSNR), Normalized correlation coefficient (NC), SSIM, BER, feature similarity (FSIM) index	Gaussian blurring, Histogram eq., Rotation, JPEG, Salt & Pepper, Gamma correction, Median filtering, JPEG, JPEG2000	The main aim of this work is to develop an effective watermarking scheme for protecting digital images against various signal processing attacks with high image quality

Table 1 (continued)

Ref. No.	Purpose	Techniques used	Input image	Performance parameters	Attacks	Remark
			Watermark: 32×32 binary logo images			
[20]	Dual image watermarking is proposed to preserve ownership rights, using critical homomorphic transform features (HT).	DWT, HT, SVD, AT	Host grayscale image: 512×512 Watermark grayscale: 512×512	PSNR, SSIM, Normalized correlation coefficient	JPEG compression, Gaussian noise, Median filter, Salt and Pepper, Low pass filter, Sharpening, Gamma correction, Scaling, Translation, Rotation,	The suggested technique is tested under multiple attacks; the simulation results demonstrate its high robustness and imperceptibility.
[18]	To protect various types of digital data from malicious attacks and to provide high robustness and imperceptibility	Homomorphic transform (HT), DWT, SVD	Host grayscale image: 512×512 Watermark grayscale: 256×256	PSNR, Normalized correlation coefficient (NCC)	Rotation, Gaussian noise, Histogram eq., Gaussian filter, Salt and Pepper, Sharpening, Average filter, Median	This approach makes the scheme blind in nature and ensures copyright protection.
[19]	To provide high imperceptibility, robustness, capacity, and security	RDWT (Redundant discrete wavelet transform), DCT (Discrete cosine transform), SVD	Host grayscale image: 512×512 Watermark grayscale: 256×256	PSNR, Normalized correlation coefficient (NCC)	Gaussian noise, Wiener filter, Salt and Pepper, Median filter, Gamma correction, Shearing,	The proposed watermarking algorithm is more robust than the existing watermarking scheme against various attacks.
[21]	The proposed method uses a cloud-based buyer-seller watermarking technology that uses a semi-trusted third party to prevent copying and maintain privacy.					
[22]	To make the watermarking scheme resistant to geometric attacks, a geometric distortion detection method based upon the quaternion Zernike moment is introduced	Quaternion Hadamard transform (QHT), Schur decomposition, Quaternion Zernike moment	Host image of size 512×512: Lena, Baboon, Boat; Watermark image of size: 64×64	SSIM, Normalized correlation coefficient	Contrast adjustment, histogram equalization, gamma correction, sharpening, filtering, Cropping, rotation, scaling	Experimental results show that the proposed scheme has not only good imperceptibility but also is robust to various kinds of attacks
[24]	A novel image watermarking method is proposed. The fruit	DWT, HD (Hessenberg decomposition),	Host grayscale image: 512×512	PSNR, MSE, SSIM (Structural similarity index	JPEG compression, Gaussian noise, median filter, Cropping,	Significant improvement in imperceptibility and

Table 1 (continued)

Ref. No.	Purpose	Techniques used	Input image	Performance parameters	Attacks	Remark
	fly optimization is used to get an optimized scaling factor	SVD, Fruit fly optimization	Watermark grayscale: 256 ×256, 128× 128, 64×64	measurement), Normalized correlation coefficient	Gaussian LPF, Rescaling, Sharpening	robustness under various attacks.
[23]	This paper presents a dual watermarking technique for color images in which robust watermarks are embedded for copyright protection	Least significant bit (LSB), DWT	Host image of size 512×512: Lena, Airplane, Baboon, Pepper, Lake, Splash, House Watermark: 64× 64	Peak signal to noise ratio (PSNR), Normalized correlation coefficient (NCC), SSIM, feature similarity (FSIM) index	Salt and Pepper, JPEG, Blurring, Gaussian noise, Darken, Twist, Resizing, Contrast	The proposed dual watermarking technique shows higher robustness and imperceptibility.
[26]	To avoid the false positive problem by integrating the watermark image's primary features and, therefore, provide copyright protection	DWT, SVD, Particle swarm optimization	Host grayscale image: 256× 256 Watermark grayscale: 128 ×128	PSNR, Normalized correlation coefficient (NCC)	Gaussian noise, Average filtering, JPEG compression, Histogram eq., Gamma correction	The proposed algorithm removes the false-positive problem and diagonal line problem
[28]	The proposed watermarking technique is used to protect data from illegal modification or reproduction	DWT, SVD	Host images: Cameraman, Cell, Circuit, MRI, Pout	MSE, PSNR, SSIM	Gaussian noise, Sharpening, Blurring, Salt and Pepper, Rotation, Cropping	Simulation results have shown that this technique can attain good imperceptibility, as the perceptual quality has not been degraded
[27]	To propose a secured, robust and imperceptible watermarking technique.	DWT, BEMD (bi-dimensional empirical mode decomposition), DCT, PSO (particle swarm optimization), and SVD	Host image of size 512×512: Barbara, baboon, cameraman, Lena, Tank, Goldhill	PSNR, MSE, NCC	Salt and pepper, Gaussian filter, rotation, median filter, speckle, gamma correction, scaling, Shearing	In comparison to the current methodologies, the proposed method offers a meaningful improvement in robustness, imperceptibility, and security.

Table 1 (continued)

Ref. No.	Purpose	Techniques used	Input image	Performance parameters	Attacks	Remark
			Watermark image of size: 128× 128			
[31]	This paper proposed a blind watermarking technique. Medical images are used for watermarking purposes. This method is proposed to provide high imperceptibility and robustness.	DWT, SVD, Region of interest (ROI)	Host images of size 1024× 1024: X-ray, CT scan; Watermark EC logo of size: 32×32	NCC, MSE, PSNR, WPSNR (Weighted PSNR)	Salt & pepper noise, Histogram equalization, Gaussian noise, Sharpening, Average filter, Resize, Cropping, JPEG compression	Analysis of the proposed scheme for color images shows that the scheme's performance is better for medical images than natural images.
[32]	To provide security, reliability, and robustness against attacks and to get an optimized scaling factor	DWT, Block SVD, Particle swarm optimization (PSO)	Host grayscale image: 512× 512 Watermark grayscale: 64× 64	PSNR, NCC, Normalized similarity ratio (NSR)	Rotation, Cropping, Gaussian noise, JPEG compression, Histogram eq., Gamma correction, Salt and Pepper	Significant improvement in imperceptibility and robustness under various attacks
[33]	This paper is proposed a significant region (SR) based image watermarking technique to design a more robust scheme against various attacks	Lifting Wavelet Transform (LWT), Random shuffling, Quantization, Block selection process	Host images of size 512× 512: Goldhill, Lena, Man, Airport, Tank, Truck, Boat, Barbara, Mandrill; Binary watermark of size 32×16	PSNR, Normalized correlation coefficient (NCC), MSE, BER	JPEG, Gaussian low pass, Histogram, Cropping, Median filter, Salt and Pepper, Gaussian noise, speckle noise, contrast Adjustment, amplification, scaling	Significant improvement in imperceptibility and robustness under various attacks
[34]	The current state of web service composition research based on bio-inspired algorithms is reviewed in this study.	Ant Colony Optimization (ACO), Genetic Algorithm (GA), Evolutionary Algorithm (EA), and Particle Swarm (PSO)	--	--	--	This study provides an overview of the research on bio-inspired algorithms in web application composition and points out future directions.

Table 1 (continued)

Ref. No.	Purpose	Techniques used	Input image	Performance parameters	Attacks	Remark
[36]	This paper proposes an algorithm for health care applications such as tele-ophthalmology, tele-medicine, etc.	DWT, DCT, SVD, Back propagation neural network	Cover image: 512 × 512 Symptoms image: 128 × 128 Record image 64 × 64	PSNR, NCC	JPEG, Salt, and Pepper, Gaussian noise, Crop, Rotation, Resize, Average filter, Low pass filter, Gamma correction	The proposed technique is suitable for preventing patient identity theft and alteration for healthcare applications.

Wavelet transform aid in developing watermarking methods while also improving computing efficiency [33]. Splitting, prediction, and updating are the three essential steps of the lifting system [29]. The block diagram is shown in Fig. 1.

Split: Lazy wavelet transform is another name for splitting. In this step, the input signal S_j is divided into even and odd samples: $S_{j,\,2k}$ and, $S_{j,\,2k\,+\,1}$ [33].

Predict: This stage can be viewed as a high-pass filtering procedure [33]. Here we predict odd samples $S_{j,\,2k\,+\,1}$ using even samples $S_{j,\,2k}$ and the abstract difference $d_{j\,-\,1}$ is generated.

Update: This step can be viewed as a low-pass filtering operation [33]. The low-frequency component $S_{j\,-\,1}$ represents a coarse approximation to the original signal S_jWhich is obtained by applying an update operator.

2.2 Discrete cosine transform (DCT)

The discrete cosine transform coefficient has only real values, unlike the discrete Fourier transform. DCT has the ability to compress an image's pixels information into a small number of DCT coefficient values, resulting in data consolidation into less values [7]. The 2D DCT and inverse DCT of an N × N image are defined as shown in Eq. (1) and Eq. (2):

$$X(i,j) = P(i)P(j)\sum_{u=0}^{N-1}\sum_{v=0}^{N-1} x(u,v)\left(cos\left[\frac{\left(u+\frac{1}{2}\right)\pi}{N}i\right]cos\left[\frac{\left(v+\frac{1}{2}\right)\pi}{N}j\right]\right) \tag{1}$$

The inverse discrete cosine transform (IDCT) in two dimensions is defined as follows [7]:

$$x(u,v) = \sum_{u=0}^{N-1}\sum_{v=0}^{N-1} P(i)P(j)\,X(i,j)\left(cos\left[\frac{(u+1/2)\pi}{N}i\right]cos\left[\frac{(v+1/2)\pi}{N}j\right]\right) \tag{2}$$

where, $P(i) = \begin{cases} \sqrt{1/N}, i = 0 \\ \sqrt{2/N}, i = 0 \end{cases}$ $P(j) = \begin{cases} \sqrt{1/N}, j = 0 \\ \sqrt{2/N}, j = 0. \end{cases}$

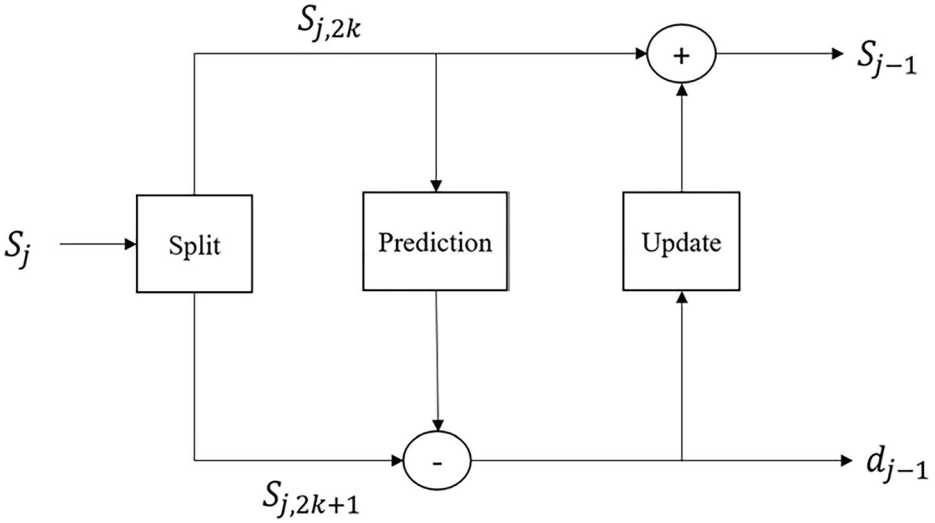

Fig. 1 Lifting wavelet decomposition

2.3 Schur decomposition (SD)

In numerical linear algebra, the Schur decomposition is a valuable technique. The Schur decomposition can be defined as shown in Eq. (3) for a real matrix H.

$$[U, D] = schur(H) \tag{3}$$

where U: unitary matrix; D: upper triangular matrix. The matrix H can be obtained as shown in Eq. (4):

$$H = U \times D \times U' \tag{4}$$

where, U' is the transpose of matrix U.

2.4 Singular value decomposition (SVD)

The N× M matrix's SVD can be written as [7]:

$$C = L \sum R^T \tag{5}$$

Where L and R are unitary orthogonal matrices shown in Eq. (6), Σ = diag (σ_1, σ_2, ⋯, σ_r, 0, ⋯, 0) is the singular value matrix, $\sigma_i = \sqrt{\lambda_i}$ (i = 1, 2, …r), and r is the rank of matrix C. The SVD is significantly used in image alteration, particularly in digital watermarking. The singular values of a matrix characterize its data distribution qualities and are reasonably stable; a slight change in the singular value does not affect the aesthetic impression of the image [25]. Furthermore, the SVD has no limit on the size of the picture matrix.

2.5 Firefly optimization

Firefly Algorithms for Multimodal Optimization is proposed by Yang [35]. Firefly algorithm can be constructed by using one of the three rules: (1) any firefly can be attracted to any other brighter one regardless of their sex, (2) The brightness of the Firefly can be determined from the encoded objective function, and (3) The attractiveness is directly proportional to brightness, and they both decreases as their distance increases. It means that the Firefly will move towards the brighter one, and if there is no brighter one, it will move randomly. From elementary physics, the light intensity is inversely proportional to the square of the distance (r). The variation of attractiveness β can be defined as shown in Eq. (6):

$$\beta(r) = \beta_o e^{-\gamma r^2} \tag{6}$$

where β_o is the attractiveness at $r = 0$. If the Firefly is located at X_j is more attractive (brighter) than another firefly located at X_iThe Firefly is located at X_i will move towards X_j. The position update of the Firefly is located at X_i can be defined as shown in Eq. (7):

$$X_i^{T+1} = X_i^T + \beta_o e^{-\gamma r^2}\left(X_j^T - X_i^T\right) + \alpha_T \in_i^T \tag{7}$$

where T is the iteration number, $\left(X_j^T - X_i^T\right)$ is the distance between the two Firefly, $\beta_o e^{-\gamma r^2}$ is the attractiveness, α_T is the constant parameter that defines randomness, and lies between 0 and 1, and $\in_i^T$ is a vector of random numbers. If $\beta_o = 0$, then it becomes a simple random walk. If

$\gamma = 0$, then it reduces to simple PSO. α_T can be defined as shown in Eq. (8):

$$\alpha_T = \alpha_o \delta^T \tag{8}$$

where α_o is the initial randomness scaling factor, and δ is essentially a cooling factor. For most of the applications $\delta = 0.95$ *to* 0.97, $\beta_o = 1$, and $\alpha_o = 0.01L$ (L = Average scale of the problem interest). However, γ, should also be related to the scaling L. In general, we can set $\gamma = \frac{1}{\sqrt{L}}$. In general, the Firefly algorithm has two inner loops when going through the population (n) and one outer loop for the iteration (T). So, the complexity in the extreme case is $O(n^2T)$. If n is very small and T is very large, the computational cost is relatively inexpensive because the algorithm complexity is linear in terms of T. Different cases of Firefly optimization are shown in Fig. 2. The flow chart of Firefly optimization is shown in Fig. 3.

2.5.1 Advantages of firefly optimization

- Firefly optimization is based on attraction, and attractiveness decreases with distance. This leads to the fact that the whole population can automatically be subdivided into subgroups.
- The parameters in Firefly can be tuned to control the randomness as iterations proceed, so that convergence can also be speed up.
- The natural capability of dealing with multimodal optimization.
- High ergodicity and diversity in the solution.

2.5.2 Working of firefly optimization

- Parameters Setting:

– Population size = 5
– Number of iterations = 20
– $\beta_o = 1, \gamma = 0.01, \delta = 0.97, \in_i^T = \left(rand - \frac{1}{2}\right) \times scale$

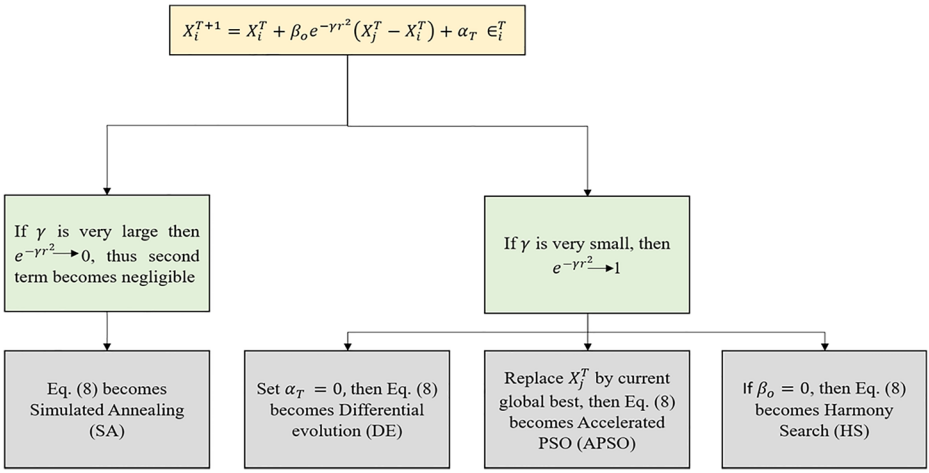

Fig. 2 Different cases of Firefly optimization

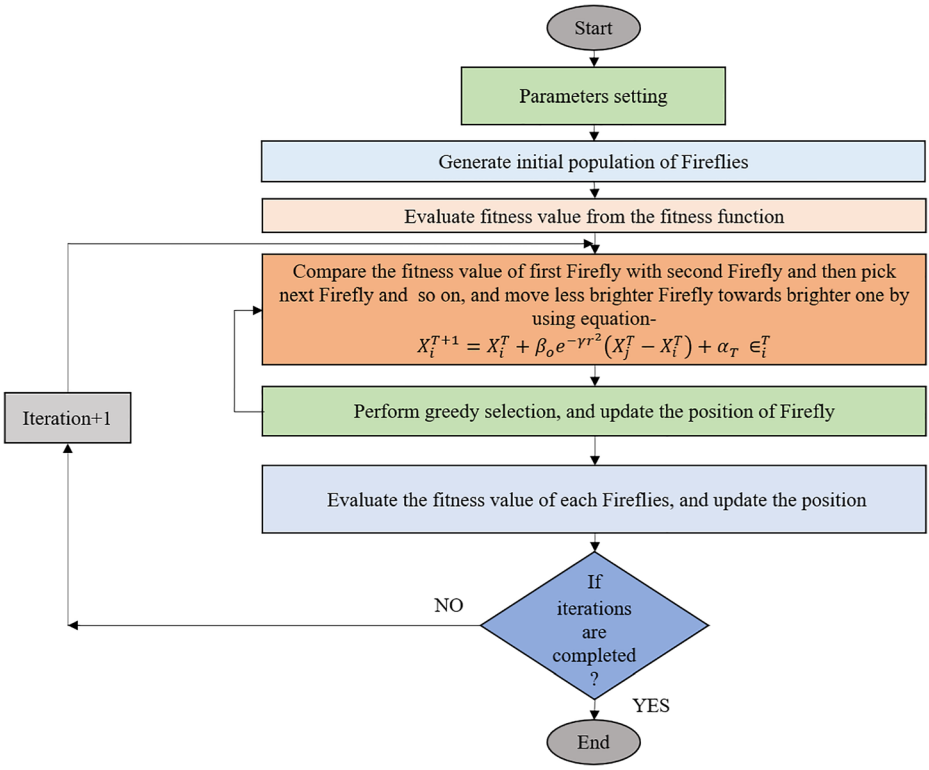

Fig. 3 Flow chart of Firefly optimization

– Dimension of the problem = 3

• Fitness function:

$$\frac{\frac{\sum_1^a NCC_1}{a} + \frac{\sum_1^a NCC_2}{a} + \frac{PSNR}{100}}{2 \times \mu + a} \tag{9}$$

In the above equation, NCC_1 is the normalized correlation coefficient for the first watermark image, NCC_2 is the normalized correlation coefficient for the second watermark image, a represents the number of attacks, and μ shows the number of used host images.

• Randomly initialize the initial position (P) of the population using Eq. (10):

$$P = Lower\ limit + rand \times (Upper\ limit - Lower\ limit) \tag{10}$$

where rand is the random number between 0 and 1, the lower limit for NCC is 0.9, and the Upper limit is 1.

- Compute the fitness value using Eq. (9) for every Firefly.
- Compare the result of the first Firefly with the second one and if the value of the first Firefly is greater than the second, then retain the old value. But if the value of the second Firefly is larger, use Eq. (7) and move the first Firefly towards the second one. This way compares the fitness value of the first Firefly with every other Firefly and updates the position if needed. Then again, compare the fitness value of every Firefly with the other one and completes the iterations.

3 Proposed watermarking algorithm

This section explains the watermarking embedding and extraction procedure. For watermarking embedding process, we have taken an Ultrasound image [size: 512 × 512] of the liver of three different patients, and two watermark logo images are used. MNNIT logo [size 256 × 256] is the first watermark image and the details of patient [size 256 × 256] are the second logo. The block diagram of the embedding and extraction algorithm is shown in Figs. 4 and 5.

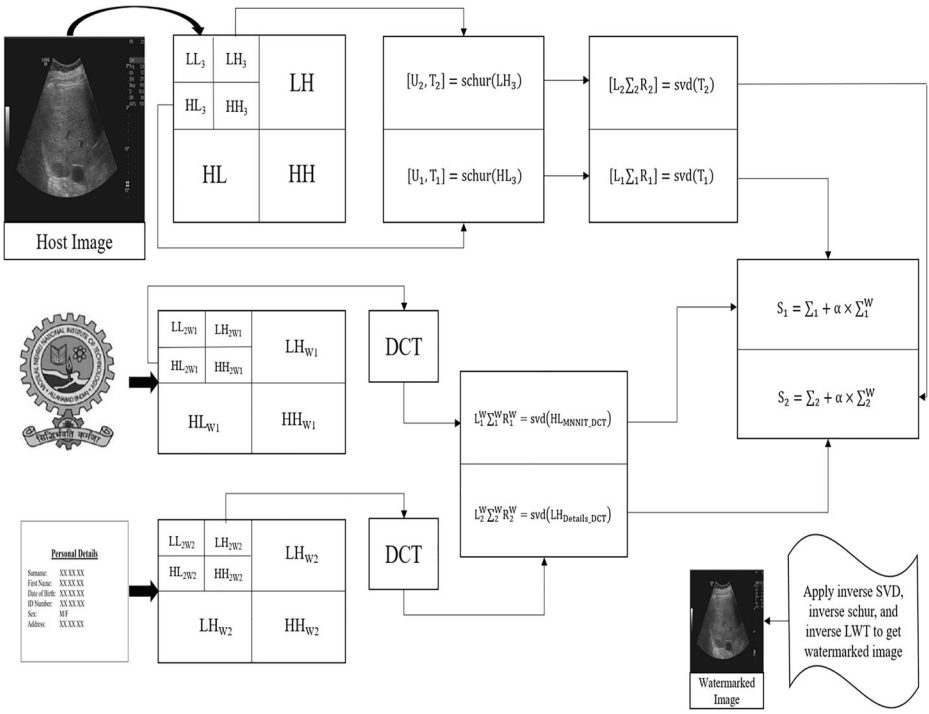

Fig. 4 Embedding Block diagram

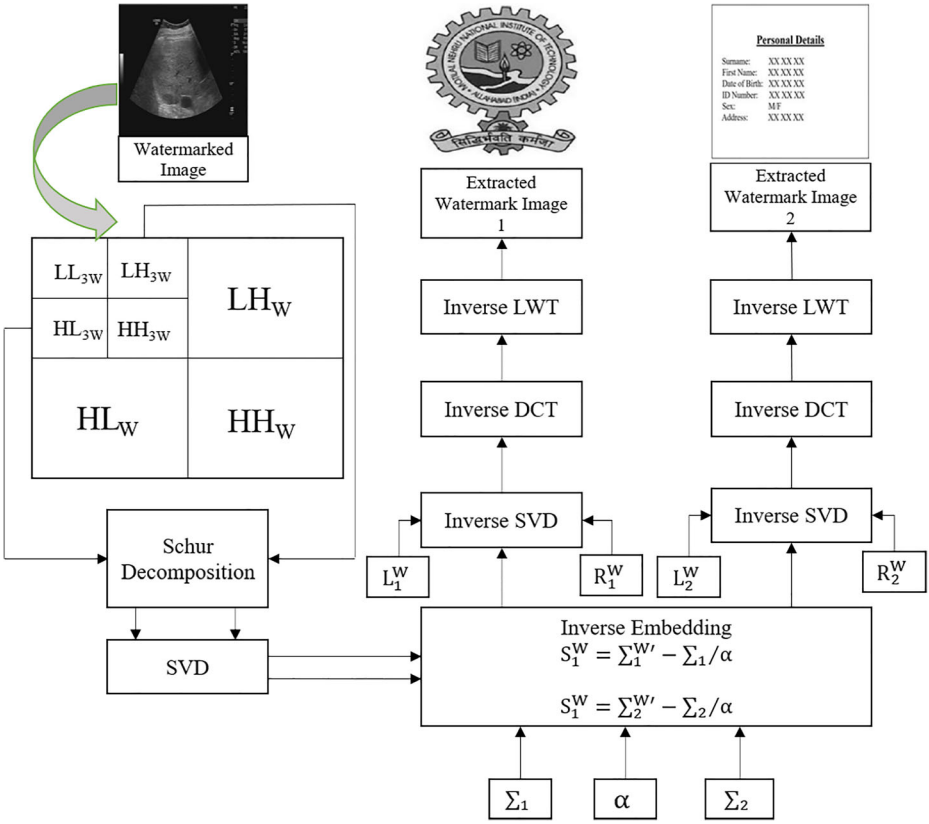

Fig. 5 Extraction Block diagram

3.1 Watermark embedding process

Step 1: Decompose the input liver ultrasound image by applying a three-level lifting wavelet transform, and pick two sub-bands (HL_3 and LH_3).

Step 2: Perform the Schur decomposition on the sub-bands to get the unitary and upper triangular matrix. In Eq. (11), U_1 is a unitary matrix, and T_1 is the upper triangular matrix for the HL_3 sub-band. In Eq. (12), U_2 is a unitary matrix, and T_2 is the upper triangular matrix for the LH_3 sub-band.

$$[U_1, T_1] = schur(HL_3) \tag{11}$$

$$[U_2, T_2] = schur(LH_3) \tag{12}$$

Step 3: Apply singular value decomposition (SVD) on the previously obtained upper triangular matrix to get the two different dominant matrices. In Eq. (13) L_1 is left unitary orthogonal matrix, R_1 is a right unitary orthogonal matrix, and $\sum_1$ is dominant matrix corresponding to T_1. In Eq. (14) L_2 is left unitary orthogonal matrix, R_2 is a right unitary orthogonal matrix, and $\sum_2$ is dominant matrix corresponding to T_1.

$$[L_1 \sum_1 R_1] = svd(T_1) \tag{13}$$

$$[L_2 \sum_2 R_2] = svd(T_2) \tag{14}$$

Step 4: Take the first watermark image: the MNNIT logo.

Step 5: Perform a two-level lifting wavelet transform on the MNNIT logo and pick the HL_{MNNIT} sub-band.

Step 6: Apply DCT on HL_{MNNIT} sub-band to get HL_{MNNIT_DCT}.
Step 7: Apply singular value decomposition after applying DCT to the obtained dominant matrix. In Eq. (15), L_1^W is left unitary orthogonal matrix, R_1^W is a right unitary orthogonal matrix, and $\sum_1^W$ is the dominant matrix corresponding to the first watermark image.

$$L_1^W \sum_1^W R_1^W = svd(HL_{MNNIT\_DCT}) \tag{15}$$

Step 8: Take the Second watermark image: Details of the patient.

Step 9: Perform two-level lifting wavelet transform on Details of the patient, and pick $LH_{Details}$ sub-band.

Step 10: Apply DCT on the $LH_{Details}$ sub-band to get $LH_{Details\_DCT}$.

Step 11: Apply singular value decomposition (SVD) after applying DCT to the obtained dominant matrix. In Eq. (16), L_2^W is left unitary orthogonal matrix, R_2^W is a right unitary orthogonal matrix, and $\sum_2^W$ is the dominant matrix corresponding to the second watermark image.

$$L_2^W \sum_2^W R_2^W = svd(LH_{Details\_DCT}) \tag{16}$$

Step 12: Add the dominant matrix of both the watermark images with the dominant matrices of the host image. In Eq. (17), α is the scaling factor, and S_1 is modified dominant matrix. In Eq. (18), α is the scaling factor, and S_2 is modified dominant matrix.

$$S_1 = \sum_1 + \alpha \times \sum_1^W \tag{17}$$

$$S_2 = \sum_2 + \alpha \times \sum_2^W \tag{18}$$

Step 12: Rebuild the sub-bands by applying inverse SVD and inverse Schur decomposition, then apply three-level inverse LWT to get the watermarked image.

3.2 Watermark extraction process

Step 1: Decompose the watermarked liver ultrasound image by applying a three-level lifting wavelet transform, and pick two sub-bands (HL_W and LH_W).

Step 2: Apply Schur decomposition on both sub-bands and then apply SVD to get two dominant matrices.

Step 3: Apply inverse embedding to both dominant matrices. In Eq. (19) S_1^W is the dominant matrix obtained after applying reverse embedding, and $\sum_1^{W'}$ is the dominant matrix of the watermarked image. In Eq. (20) S_2^W is the dominant matrix obtained after applying reverse embedding, and $\sum_2^{W'}$ is the dominant matrix of the watermarked image.

$$S_1^W = \left(\sum_1^{W'} - \sum_1\right)/\alpha \tag{19}$$

$$S_1^W = \left(\sum_2^{W'} - \sum_2\right)/\alpha \tag{20}$$

Step 4: Apply inverse SVD and DCT on previously obtained inverse embed dominant matrices.

Step 5: Apply the two-level inverse lifting Wavelet transform to get the extracted watermark.

P1 P2 P3

Fig. 6 Host images: P1-Patient 1, P2-Patient 2, P3-Patient 3

4 Results and discussion

The proposed algorithm is implemented with the help of MATLAB R2017a installed in the system with specifications as Lenovo 11th generation Intel(R) Core (TM) i5-1135G7 @ 2.40GHz - 2.42 GHz. The proposed watermarking method is tested on an Ultrasound image [size: 512 × 512] of the liver of three different patients taken from the cancer imaging archive [11], shown in Fig. 6, and two watermark logo images are used, shown in Fig. 7. MNNIT logo [size 256 × 256] is the first watermark image, and the details of patient [size 256 × 256] are the second logo. The watermarked image is shown in Fig. 8, and extracted watermark logo is shown in Fig. 9. To check the performance of the proposed method, the peak signal to noise ratio (PSNR), structural similarity index measurement (SSIM), and normalized correlation coefficient (NCC1 is used for MNNIT logo, and NCC2 is used for Details of patient image). The PSNR and SSIM value is used for the imperceptibility of the proposed method, and NCC is used for robustness. Table 2 shows the PSNR, SSIM, and NCC values for different host images without attack. The PSNR value for patient 1 is 45.8168, patient 2 is 45.7966, and patient 3 is 45.8186. The PSNR value is highest for patient 3. The SSIM value for patient 1 is 0.9969, patient 2 is 0.9951, and patient 3 is 0.9967. The PSNR value is highest for patient 1. The performance parameters are shown in Eqs. (22), (23), (24), and (25).

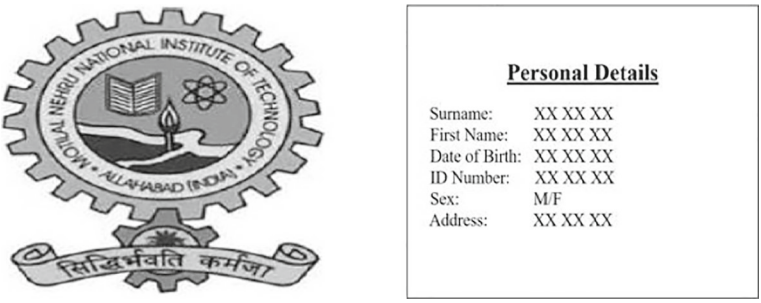

W1 W2

Fig. 7 Watermark images: W1-Watermark 1 (MNNIT logo), W2-Watermark 2 (Details of Patient)

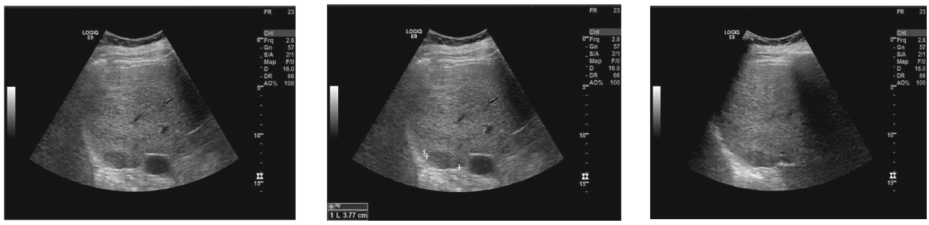

Fig. 8 Watermarked images: WP1- Watermarked Patient 1, WP2-Watermarked Patient 2, WP3-Watermarked Patient 3

4.1 Performance parameters

The proposed scheme uses the PSNR value to comment on imperceptibility.

$$PSNR = 10log_{10}\left(\frac{Pixel^2}{MSE}\right) \tag{21}$$

Pixel is the maximum pixel value in the above equation, and *MSE* is the mean square error value. Mean square error (*MSE*) can be defined as:

$$MSE = \frac{\sum_{i=0}^{M-1}\sum_{j=0}^{N-1}[H_I(i,j) - W_I(i,j)]^2}{M \times N} \tag{22}$$

where $M \times N$ is the size of the host image, $H_I(i,j)$ is the host image, $W_I(i,j)$ is the watermarked image, and i, j is used for pixels.

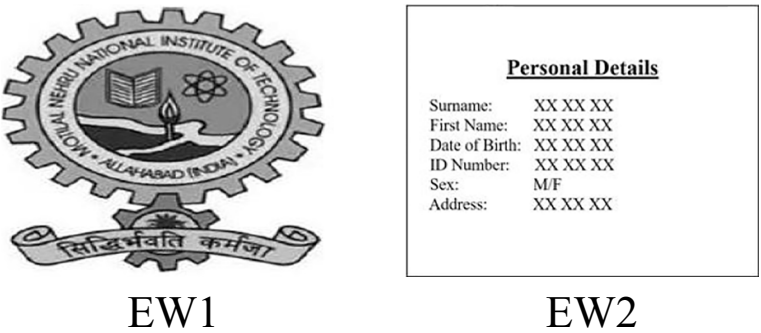

Fig. 9 Extracted watermark images: EW1-Extracted watermark 1 (MNNIT logo), EW2- Extracted watermark 2 (Details of Patient)

Table 2 PSNR, SSIM, and NCC values for different host images without attack

Host Image	PSNR (dB)	SSIM	NCC1	NCC2
P1	45.8168	0.9969	1.0000	1.0000
P2	45.7966	0.9951	1.0000	1.0000
P3	45.8186	0.9967	1.0000	1.0000

Table 3 PSNR, SSIM, and NCC values for P1 host image under attacks

Attacks	PSNR (dB)	SSIM	NCC1	NCC2
Salt and Pepper noise (0.001)	34.7385	0.9751	0.9998	0.9999
Gaussian noise (0,0.001)	30.8709	0.9716	0.9995	0.9994
Speckle noise (0.02)	26.2916	0.7133	0.9971	0.9984
Gaussian low pass filter (3 × 3)	45.1891	0.9937	0.9995	0.9998
Average filter (3 × 3)	38.9229	0.9851	0.9957	0.9981
Median filter (3 × 3)	43.0525	0.9883	0.9997	0.9999
Rotation (2)	12.5608	0.6203	0.9950	0.9958
Histogram eq.	11.7571	0.5618	0.9845	0.9861
Sharpening	31.7900	0.9758	0.9730	0.9876
Wiener filter (3 × 3)	42.5133	0.9870	0.9989	0.9995
JPEG (90)	43.9055	0.9928	0.9994	0.9998
JPEG 2000 (10)	45.1019	0.9924	0.9996	0.9998
Motion blur	35.8291	0.9760	0.9982	0.9921
Shearing	12.2016	0.6012	0.9870	0.9816
Region of interest filtering	44.7626	0.9918	1.0000	1.0000

Structural similarity index measurement (*SSIM*) is also used to comment on the imperceptibility of the proposed watermarking scheme and is defined as:

$$SSIM(x,y) = \frac{\left(2\mu_x\mu_y + C_1\right)\left(2\sigma_{xy} + C_2\right)}{\left(\mu_x^2 + \mu_y^2 + C_1\right)\left(\sigma_x^2 + \sigma_y^2 + C_2\right)} \tag{23}$$

where μ_x, μ_y, σ_x, σ_y, and σ_{xy} are the local means, standard deviations, and cross-covariance for images *x, y, and* C_1 *and* C_2 *are the regularization constant for the luminance and contrast.*

Table 4 PSNR, SSIM, and NCC values for P2 host image under attacks

Attacks	PSNR (dB)	SSIM	NCC1	NCC2
Salt and Pepper noise (0.001)	35.2279	0.9667	0.9999	1.0000
Gaussian noise (0,0.001)	30.4923	0.9630	0.9999	0.9999
Speckle noise (0.02)	21.9830	0.8146	0.9978	0.9985
Gaussian low pass filter (3 × 3)	42.3107	0.9845	0.9998	0.9999
Average filter (3 × 3)	33.9608	0.9637	0.9981	0.9990
Median filter (3 × 3)	41.7102	0.9873	0.9993	0.9997
Rotation (2)	15.8857	0.5843	0.9430	0.9703
Histogram eq.	20.9272	0.8102	0.9917	0.9884
Sharpening	35.9569	0.9410	0.9864	0.9947
Wiener filter (3 × 3)	43.9449	0.9878	0.9998	0.9996
JPEG (90)	44.3145	0.9908	0.9999	1.0000
JPEG 2000 (10)	45.2125	0.9938	1.0000	1.0000
Motion blur	32.8780	0.9555	0.9991	0.9961
Shearing	11.5788	0.4518	0.9964	0.9718
Region of interest filtering	45.1307	0.9948	1.0000	1.0000

Table 5 PSNR, SSIM, and NCC values for P3 host image under attacks

Attacks	PSNR (dB)	SSIM	NCC1	NCC2
Salt and Pepper noise (0.001)	34.5093	0.9726	1.0000	0.9999
Gaussian noise (0,0.001)	30.5798	0.6763	0.9999	0.9998
Speckle noise (0.02)	27.6779	0.7993	0.9994	0.9992
Gaussian low pass filter (3 × 3)	43.0262	0.9938	0.9998	0.9997
Average filter (3 × 3)	35.3777	0.9642	0.9982	0.9975
Median filter (3 × 3)	38.5289	0.9734	0.9995	0.9996
Rotation (2)	14.1548	0.5840	0.9924	0.9970
Histogram eq.	10.4261	0.4135	0.9493	0.9842
Sharpening	31.0042	0.8947	0.9879	0.9827
Wiener filter (3 × 3)	40.3403	0.9728	0.9993	0.9997
JPEG (90)	42.8298	0.9862	1.0000	1.0000
JPEG 2000 (10)	44.8913	0.9943	1.0000	1.0000
Motion blur	30.4943	0.9090	0.9988	0.9883
Shearing	13.0938	0.4119	0.9960	0.9821
Region of interest filtering	41.7626	0.9923	0.9999	0.9999

This paper uses normalized correlation coefficient (*NCC*) values to comment on the robustness of the proposed watermarking scheme and is defined as:

$$NCC = \frac{\sum_{i=0}^{M-1}\sum_{j=0}^{N-1} W(i,j)W_r(\mathrm{i},j)}{\sqrt{\sum_{i=0}^{M-1}\sum_{j=0}^{N-1} W^2(i,j)}\sqrt{\sum_{i=0}^{M-1}\sum_{j=0}^{N-1} {W_r}^2(i,j)}} \tag{24}$$

where $W(i,j)$ is the original watermark logo, and $W_r(i,j)$ is the recovered watermark logo.

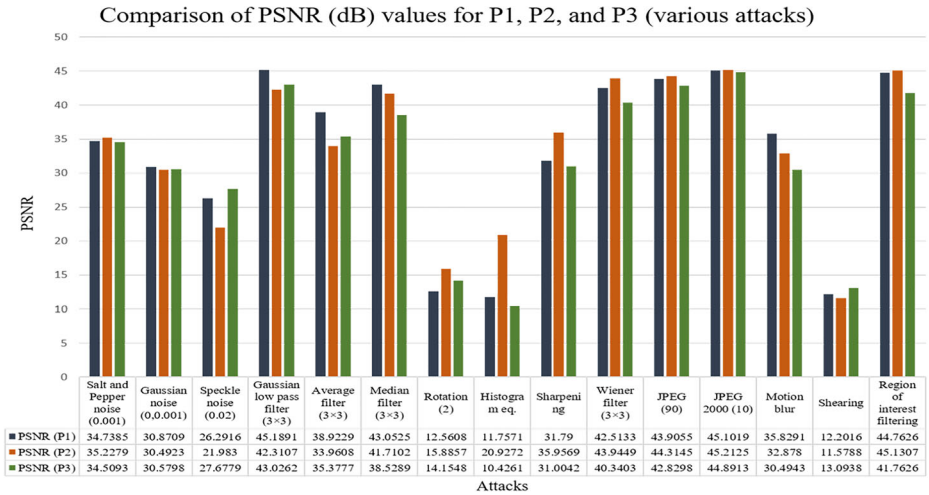

Fig. 10 Comparison of PSNR values for P1, P2, and P3 (various attacks)

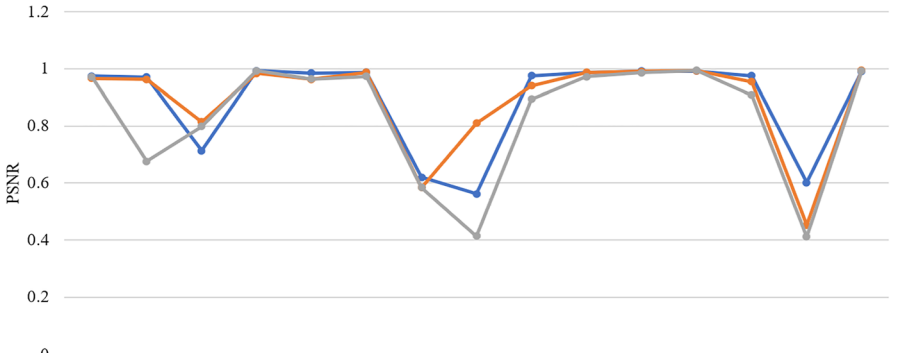

	Salt and Pepper noise (0.001)	Gaussian noise (0,0.001)	Speckle noise (0.02)	Gaussian low pass filter (3×3)	Average filter (3×3)	Median filter (3×3)	Rotation (2)	Histogram eq.	Sharpening	Wiener filter (3×3)	JPEG (90)	JPEG 2000 (10)	Motion blur	Shearing	Region of interest filtering
SSIM (P1)	0.9751	0.9716	0.7133	0.9937	0.9851	0.9883	0.6203	0.5618	0.9758	0.987	0.9928	0.9924	0.976	0.6012	0.9918
SSIM (P2)	0.9667	0.963	0.8146	0.9845	0.9637	0.9873	0.5843	0.8102	0.941	0.9878	0.9908	0.9938	0.9555	0.4518	0.9948
SSIM (P3)	0.9726	0.6763	0.7993	0.9938	0.9642	0.9734	0.584	0.4135	0.8947	0.9728	0.9862	0.9943	0.909	0.4119	0.9923

Attacks

Fig. 11 Comparison of SSIM values for P1, P2, and P3 (various attacks)

4.2 Imperceptibility analysis

The invisibility of the proposed scheme is determined by the PSNR. Table 3 shows the PSNR and SSIM values P1 host image under attacks. The PSNR value for Salt and Pepper noise (0.001) is 34.7385, Gaussian noise (0,0.001) is 30.8709, Speckle noise (0.02) is 26.2916, Gaussian low pass filter (3 × 3) is 45.1891, Average filter (3 × 3) is 38.9229, Median filter (3 × 3) is 43.0525, Sharpening is 31.7900, Wiener filter (3 × 3) is 42.5133, JPEG (90) is 43.9055, JPEG 2000 (10) is 45.1019, Motion blur is 35.8291, and Region of interest filtering is 44.7626. The highest PSNR value is for JPEG 2000 (10). The PSNR value for Rotation (2) is 12.5608, Histogram eq. is 11.7571, and Shearing is 12.2016. The lowest value of PSNR is for Histogram eq. The highest value of SSIM is for Gaussian low pass filter (0.9937), and the lowest value is for Histogram eq. (0.5618).

Parents (calling functions)
No parent

Lines where the most time was spent

Line Number	Code	Calls	Total Time	% Time	Time Plot
12	imshow(IIII,[]);	1	1.336 s	34.6%	
31	imshow(IW1);	1	0.311 s	8.1%	
6	info=dicominfo('C:\Users\DIVYA...	1	0.251 s	6.5%	
11	figure(1)	1	0.203 s	5.3%	
46	imshow(IW2);	1	0.189 s	4.9%	
All other lines			1.567 s	40.6%	
Totals			3.857 s	100%	

(a)

Children (called functions)

Function Name	Function Type	Calls	Total Time	% Time	Time Plot
imshow	function	4	1.981 s	51.4%	
dicominfo	function	1	0.195 s	5.0%	
iwt2	function	7	0.151 s	3.9%	
dct2	function	2	0.126 s	3.3%	
imresize	function	3	0.117 s	3.0%	
imread	function	2	0.097 s	2.5%	
dicomread	function	1	0.067 s	1.7%	
imwrite	function	1	0.056 s	1.5%	
iwt2	function	3	0.030 s	0.8%	
title	function	4	0.022 s	0.6%	
close	function	1	0.021 s	0.6%	
rgb2gray	function	3	0.005 s	0.1%	
im2double	function	3	0.005 s	0.1%	
LoginCefWindow>LoginCefWindow.delete	class method	1	0.001 s	0.0%	
Self time (built-ins, overhead, etc.)			0.983 s	25.5%	
Totals			3.857 s	100%	

(b)

Fig. 12 **a** Time analysis of Parent calling functions **b** Time analysis of Children calling functions

Profile Summary

Generated 20-May-2022 10:14:31 using performance time.

Function Name	Calls	Total Time	Self Time*	Total Time Plot (dark band = self time)
dicom_new	1	3.857 s	0.983 s	
imshow	4	1.981 s	0.307 s	
initSize	4	0.978 s	0.086 s	
movegui	4	0.711 s	0.705 s	
newplot	8	0.511 s	0.451 s	
dicominfo	1	0.195 s	0.023 s	
lwt2	7	0.151 s	0.065 s	
figparams	4	0.149 s	0.059 s	
dct2	2	0.126 s	0.016 s	
imresize	3	0.117 s	0.031 s	
dicominfo>parseSequence	1	0.112 s	0.003 s	
images\private\dct	4	0.111 s	0.111 s	
imread	2	0.097 s	0.014 s	
basicImageDisplay	4	0.093 s	0.065 s	
close	2	0.090 s	0.003 s	
dicominfo>processMetadata	9	0.076 s	0.006 s	
dicominfo>convertRawAttr	86	0.070 s	0.022 s	
imread>call_format_specific_reader	2	0.069 s	0.004 s	
dicomread	1	0.067 s	0.001 s	
close>request_close	2	0.067 s	0.009 s	
dicomread>newDicomread	1	0.066 s	0.003 s	
imagesci\private\readjpg	2	0.066 s	0.014 s	
liftwave	10	0.058 s	0.029 s	
imwrite	1	0.056 s	0.015 s	
imageDisplayParseInputs	4	0.054 s	0.030 s	
dicominfo>createMetadataStruct	9	0.054 s	0.017 s	
newplot>ObserveAxesNextPlot	8	0.052 s	0.012 s	

Fig. 13 Profile Summary

Table 4 shows the PSNR and SSIM values P2 host image under attacks. The PSNR value for Salt and Pepper noise (0.001) is 35.2279, Gaussian noise (0,0.001) is 30.4923, Speckle noise (0.02) is 21.9830, Gaussian low pass filter (3 × 3) is 42.3107, Average filter (3 × 3) is 33.9608, Median filter (3 × 3) is 41.7102, Sharpening is 35.9569, Wiener filter (3 × 3) is 43.9449, JPEG (90) is 44.3145, JPEG 2000 (10) is 45.2125, Motion blur is 32.8780, and Region of interest filtering is 45.1307. The highest PSNR value is for Region of interest filtering. The PSNR value for Rotation (2) is 15.8857, Histogram eq. is 20.9272, and Shearing is 11.5788. The lowest value of PSNR is for Shearing. The highest value of SSIM is for Region of interest filtering (0.9948), and the lowest value is for Shearing (0.4518).

Table 5 shows the PSNR and SSIM values P3 host image under attacks. The PSNR value for Salt and Pepper noise (0.001) is 34.5093, Gaussian noise (0,0.001) is 30.5798, Speckle

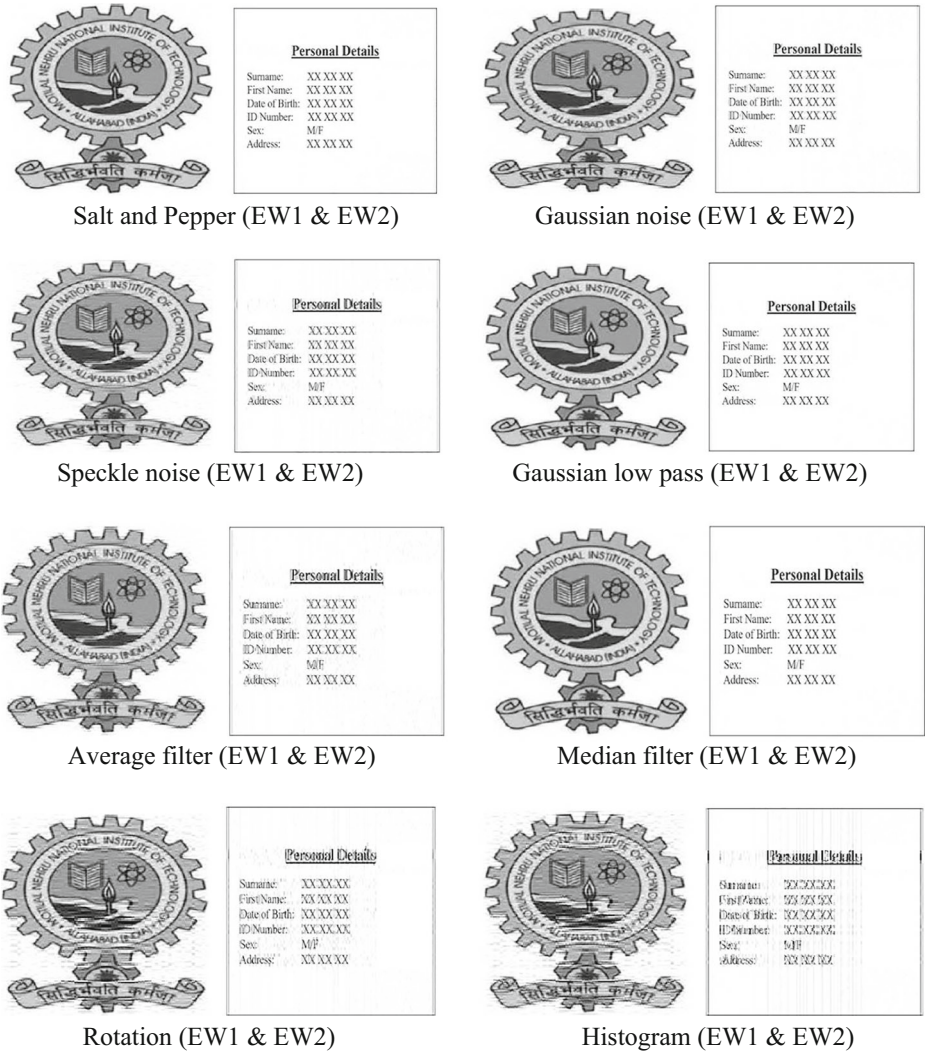

Fig. 14 Extracted watermark images for P1

noise (0.02) is 27.6779, Gaussian low pass filter (3 × 3) is 43.0262, Average filter (3 × 3) is 35.3777, Median filter (3 × 3) is 38.5289, Sharpening is 31.0042, Wiener filter (3 × 3) is 40.3403, JPEG (90) is 42.8298, JPEG 2000 (10) is 42.8298, Motion blur is 30.4943, and Region of interest filtering is 41.7626. The highest PSNR value is for JPEG 2000 (10). The PSNR value for Rotation (2) is 14.1548, Histogram eq. is 10.4261, and Shearing is 13.0938. The lowest value of PSNR is for Histogram eq. The highest value of SSIM is for JPEG 2000 (10) (0.9944), and the lowest value is for Shearing (0.4119). The Comparison of PSNR values for P1, P2, and P3 is shown in Fig. 10. The Comparison of SSIM values for P1, P2, and P3 is shown in Fig. 11 and the timing analysis is shown if Figs. 12 and 13.

Sharpening filter (EW1 & EW2)

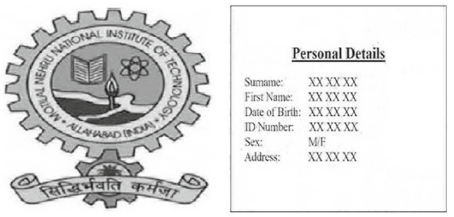

Wiener filter (EW1 & EW2)

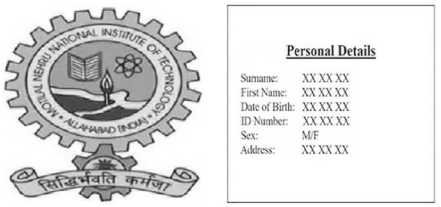

JPEG (EW1 & EW2)

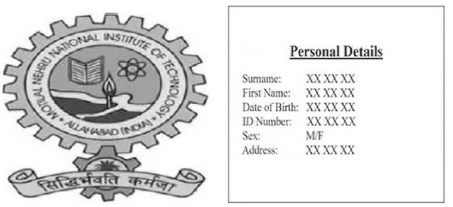

JPEG2000 (EW1 & EW2)

Motion blur (EW1 & EW2)

Shearing (EW1 & EW2)

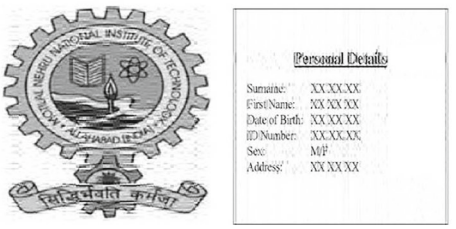

Region of interest filter (EW1 & EW2)

Fig. 14 (continued)

4.3 Robustness analysis

The robustness of the proposed scheme is determined by the normalized correlation coefficient. NCC1 is used for the MNNIT logo, and NCC2 is used for Details of patient image. Table 3 shows the NCC1 and NCC2 values for P1. NCC1 and NCC2 values are the highest for Region of interest filtering (1.0000). The NCC1 value is lowest for sharpening (0.9730), and the NCC2 value is lowest for Shearing (0.9816). Table 4 shows the NCC1 and NCC2 values for P2. NCC1 and NCC2 values are highest for Region of interest filtering (1.0000) and JPEG

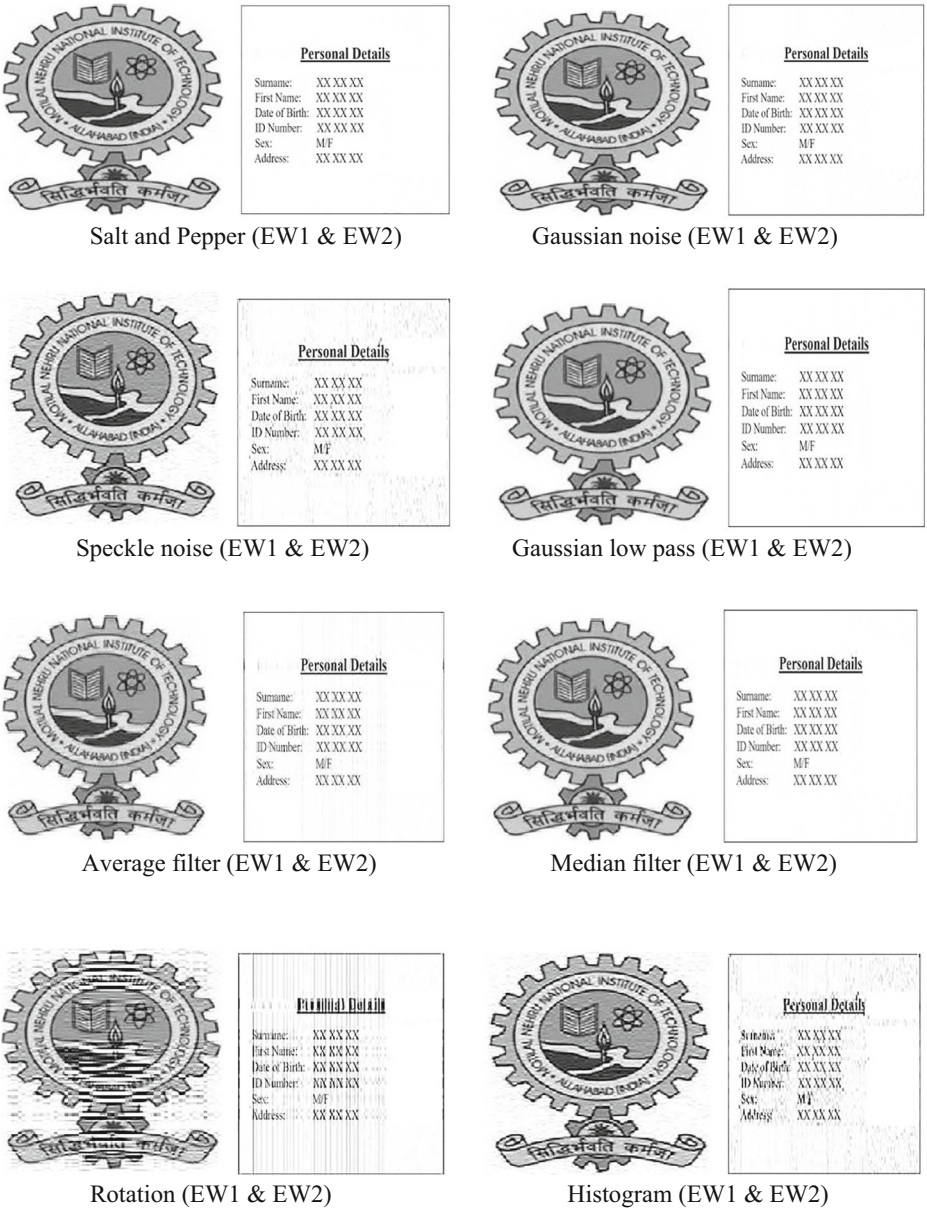

Fig. 15 Extracted watermark images for P2

2000 (1.0000). The NCC1 value is lowest for rotation (0.9430), and the NCC2 value is lowest for rotation (0.9703). Table 5 shows the NCC1 and NCC2 values for P3. NCC1 value is highest for Salt and Pepper noise (1.0000), JPEG (1.0000), and JPEG 2000 (1.0000). NCC2 value is highest for JPEG (1.0000) and JPEG 2000 (1.0000). The NCC1 value is lowest for histogram (0.9493), and the NCC2 value is lowest for Shearing (0.9821). The extracted watermark logo images for P1, P2 and P3 are shown in Figs. 14, 15 and 16, respectively.

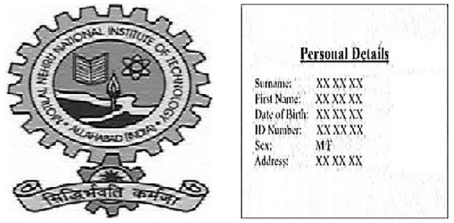

Sharpening filter (EW1 & EW2)

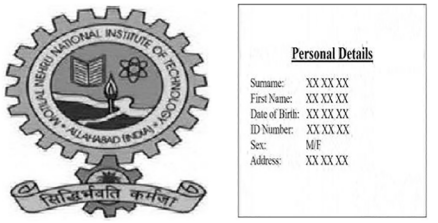

Wiener filter (EW1 & EW2)

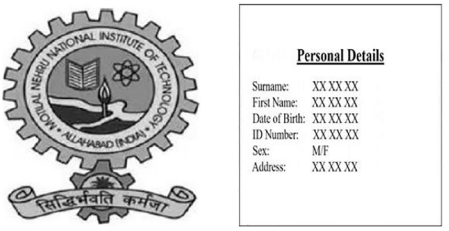

JPEG (EW1 & EW2)

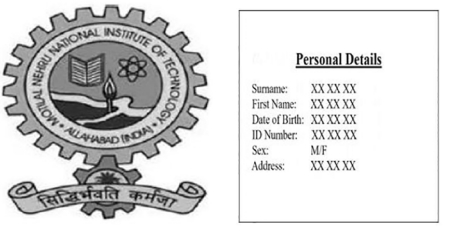

JPEG2000 (EW1 & EW2)

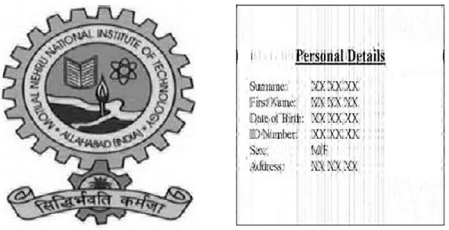

Motion blur (EW1 & EW2)

Shearing (EW1 & EW2)

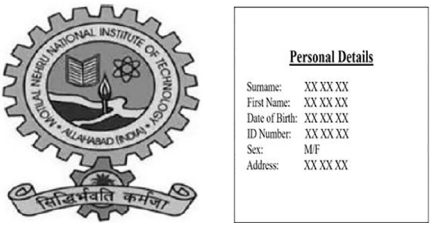

Region of interest filter (EW1 & EW2)

Fig. 15 (continued)

4.4 Time analysis

Profiling is a technique for determining how long our code to run entirely takes and where MATLAB invests the most time. After determining which functions take the most time, we may assess them for potential performance enhancements. Figures 12 and 13 show the timing analysis of the algorithm. Function name: The function that the profiled code calls.Calls: The number of incidents the function was called by the profiled code.Total Time: In seconds, the overall time spent in the function. Time spent on child functions is included in the function

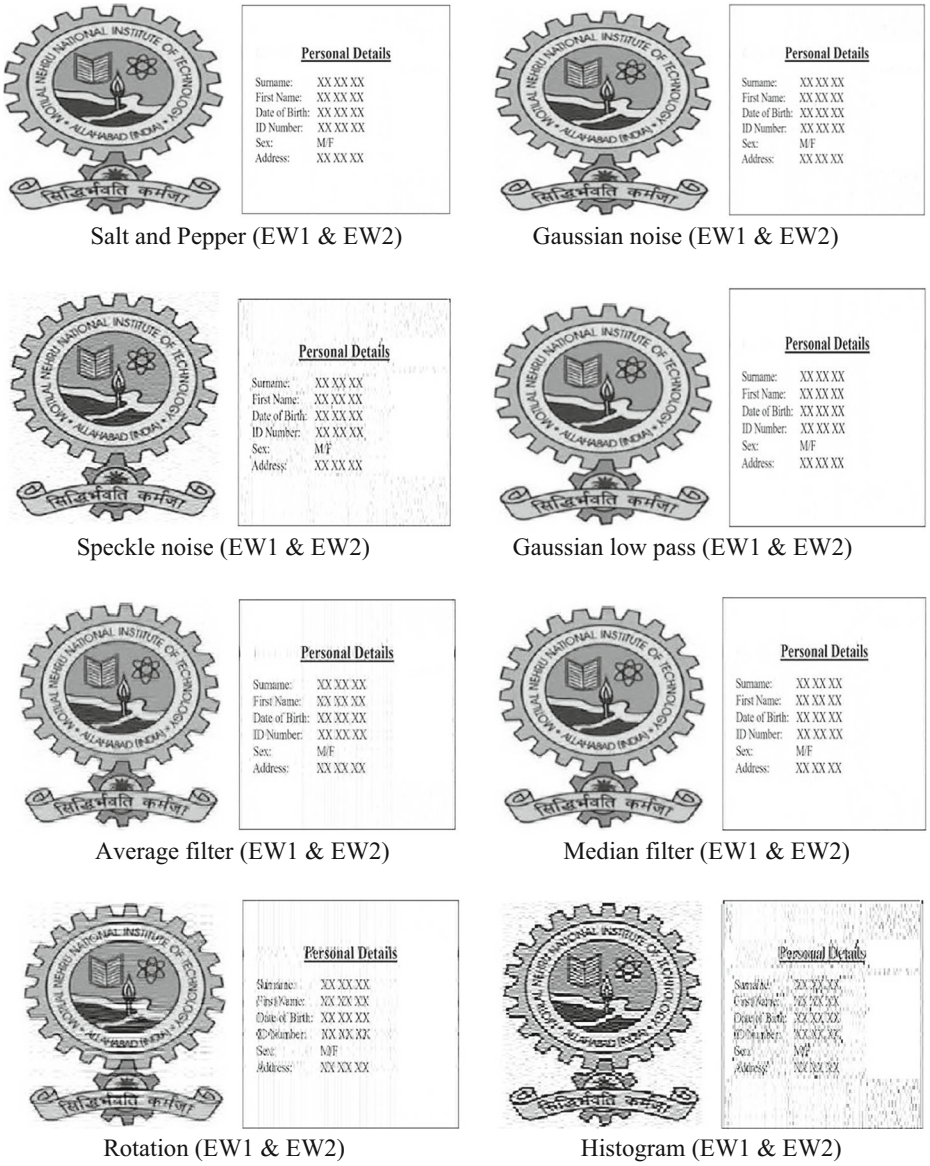

Salt and Pepper (EW1 & EW2) Gaussian noise (EW1 & EW2)

Speckle noise (EW1 & EW2) Gaussian low pass (EW1 & EW2)

Average filter (EW1 & EW2) Median filter (EW1 & EW2)

Rotation (EW1 & EW2) Histogram (EW1 & EW2)

Fig. 16 Extracted watermark images for P3

time. The Profiler takes some time, which is reflected in the final results. For files with insignificant run times, the total duration can be nil.Self-Time: Time spent in a function in seconds, discounting time invested in any child functions. Self-time contains some overhead incurred during the profiling procedure.

The dual image watermarking increases the security of the proposed watermarking technique. The proposed technique is highly robust against various attacks. The imperceptibility of the proposed scheme is also up to the mark. The firefly optimization is used to get the

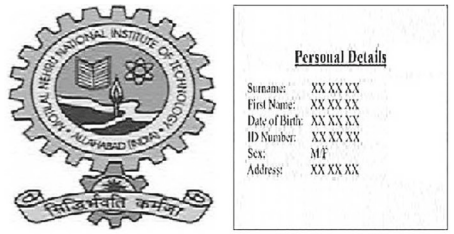

Sharpening filter (EW1 & EW2)

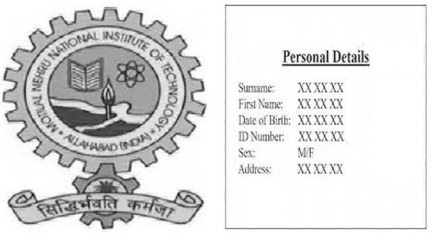

Wiener filter (EW1 & EW2)

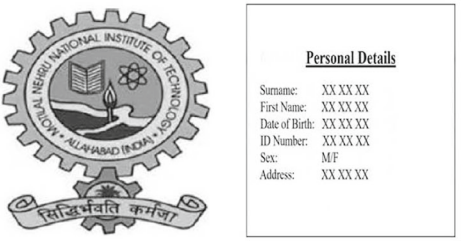

JPEG (EW1 & EW2)

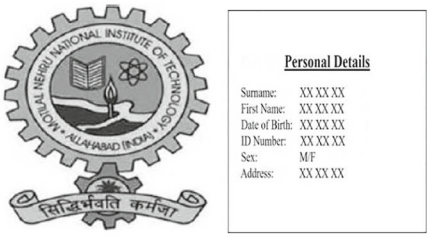

JPEG2000 (EW1 & EW2)

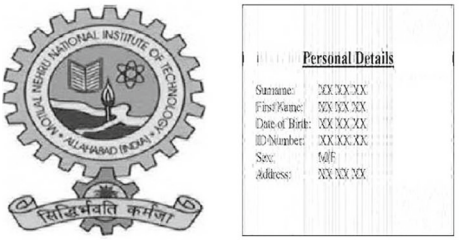

Motion blur (EW1 & EW2)

Shearing (EW1 & EW2)

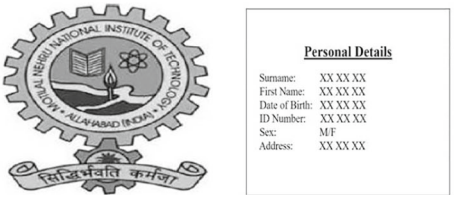

Region of interest filter (EW1 & EW2)

Fig. 16 (continued)

optimized scaling factor. The timing complexity is significantly less and the proposed scheme takes lesser time to implement. The SURF features successfully matches the concerned portions of the given medical image and there is no significant distortion in these portions.

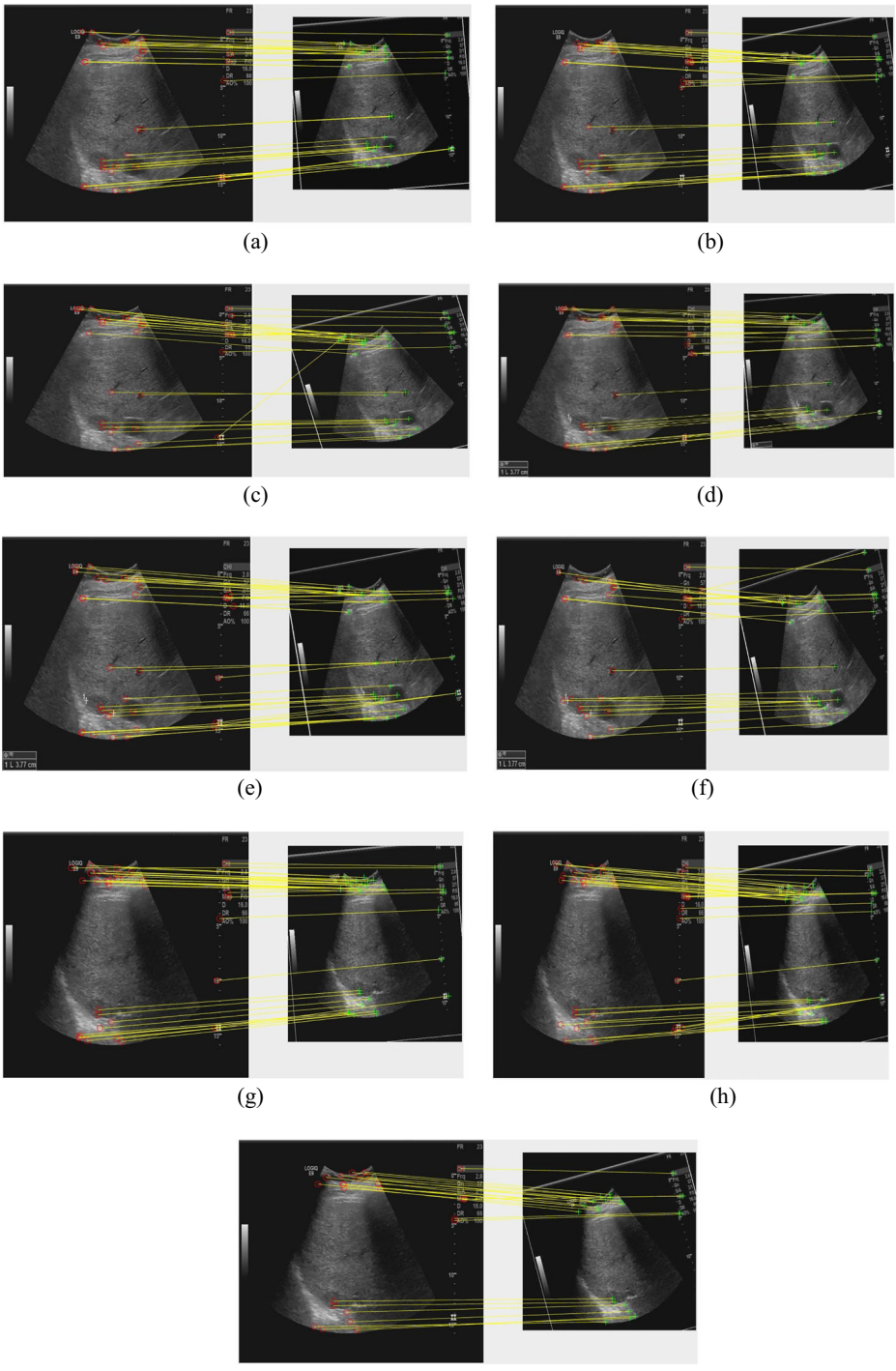

Fig. 17 Matched features (**a**) Rotation 5 (P1) (**b**) Rotation 10 (P1) (**c**) Rotation 15 (P1) (**d**) Rotation 5 (P2) (**e**) Rotation 10 (P2) (**f**) Rotation 15 (P2) (**g**) Rotation 5 (P3) (**h**) Rotation 10 (P3) (**i**) Rotation 15 (P3)

Table 6 Matched features using SURF

Rotation in degrees	Matched Features (P1)	Matched Features (P2)	Matched Features (P3)
5	36	32	33
10	33	33	36
15	33	26	24

5 SURF Feature Extraction & Matching

SURF is an enhancement on SIFT as an image key point definition operator depending on scale space. The SURF operator's graphic features resist noise, filtering, and rotation. The Hessian matrix is used by the SURF technique to find extreme points. In feature extraction, the SURF method uses box filtering rather than Gauss filtering. Simple addition and deduction can be used to finish the image filtering operation. In Fig. 17, matched features between the original image and rotated images are shown. The performance of the efficient algorithm SURF is identical to that of SIFT, but its computational complexity is lower. The SIFT algorithm shows its strength in the majority of circumstances, but its performance is still sluggish. The SURF algorithm is similar to SIFT and it also performs well (Table 6).

In Fig. 13, the ultrasound image of the liver is shown. In all the images, the black portion represents the presence of fluid, and the white part shows the presence of fat. There is a concentration of black portion, i.e., fluid in all the images in some parts. So, these two points are mainly the concerns of this medical image. With the help of SURF, the features of these two portions are extracted, even after taking one of the image as a rotated watermarked image. It is clear from the above images that the concerned portions of the used DICOM medical image are not changed or distorted because the SURF feature matches these portions, and there is no error in matching.

6 Conclusion

In the proposed scheme, a dual image watermarking technique is proposed, which utilizes the properties of Schur decomposition, SVD-DCT-LWT for embedding to improve the robustness and imperceptibility and to further improve the performance of the scheme firefly optimization is used. SURF features are used for authentication. The SURF features successfully matches the Region of interest of the given DICOM medical image and there is no distortion or alteration to these portions. The security of the scheme is also increased due to the use of dual image watermarking. The proposed watermarking method is robust against various attacks like Salt and Pepper noise, Speckle noise, Gaussian noise, Gaussian low pass filter, Average filter, Median filter, Rotation, Histogram, Motion blur, and Region of interest filter. The PSNR values for different input images are greater than 40 dB (without attack), the PSNR values for salt and pepper noise, Gaussian noise, Gaussian low pass filter, Average filter, Median filter, Sharpening, Wiener filter, JPEG, JPEG 2000, Motion blur and Region of interest filtering are greater than 30 dB except for Rotation, Histogram equalization and Shearing. By observing the PSNR values, it shows that the imperceptibility or invisibility of the proposed watermarking scheme is improved. The proposed technique can further be improved by using machine learning techniques for feature matching or authentication. The security of the scheme for medical data can be improved by using encryption techniques.

Data availability The datasets generated during and/or analyzed during the current study are available from the corresponding author on reasonable request.

Declarations

Competing interests No funds, grants, or other support were received. The authors have no competing interests to declare that are relevant to the content of this article.

References

1. Abdulrahman AK, Ozturk S (2019) A novel hybrid DCT and DWT based robust watermarking algorithm for color images. Multimed Tools Appl 78(12):17027–17049
2. Ahmaderaghi B, Kurugollu F, Del Rincon JM, Bouridane A (2018) Blind image watermark detection algorithm based on discrete shearlet transform using statistical decision theory. IEEE Trans Comput Imaging 4(1):46–59
3. Amirgholipour SK, Naghsh-Nilchi AR (2009) Robust digital image watermarking based on joint DWT-DCT. Int J Digit Content Technol Appl 3(2):42–54
4. Amrit P, Singh AK (2022) Survey on watermarking methods in the artificial intelligence domain and beyond. Comput Commun 188:52–65
5. Anand A, Singh AK (2022) Dual watermarking for security of COVID-19 patient record. IEEE Trans Dependable Secure Comput:1. https://doi.org/10.1109/TDSC.2022.3144657
6. Aslantas V (2008) A singular-value decomposition-based image watermarking using genetic algorithm. AEU-Int J Electron Commun 62(5):386–394
7. Awasthi D, Srivastava VK (2022) LWT-DCT-SVD and DWT-DCT-SVD based watermarking schemes with their performance enhancement using Jaya and Particle swarm optimization and comparison of results under various attacks. *Multimed Tools Appl* 81:25075–25099
8. Bao P, Ma X (2005) Image adaptive watermarking using wavelet domain singular value decomposition. IEEE Trans Circuits Syst Video Technol 15(1):96–102
9. Bhatnagar G, Raman B, Swaminathan K (2008, August) DWT-SVD based dual watermarking scheme. In: *2008 first international conference on the applications of digital information and web technologies (ICADIWT)*. IEEE. pp. 526-531
10. Chang TJ, Pan IH, Huang PS, Hu CH (2019) A robust DCT-2DLDA watermark for color images. Multimed Tools Appl 78(7):9169–9191
11. Clark K, Vendt B, Smith K, Freymann J, Kirby J, Koppel P, Moore S, Phillips S, Maffitt D, Pringle M, Tarbox L, Prior F (2013) The Cancer imaging archive (TCIA): maintaining and operating a public information repository. J Digit Imaging 26(6):1045–1057
12. Dowling J, Planitz BM, Maeder AJ, Du J, Pham B, Boyd C, ..., Crozier S (2007, December) A comparison of DCT and DWT block-based watermarking on medical image quality. In: *International Workshop on Digital Watermarking* (pp. 454–466). Springer, Berlin, Heidelberg., 2008
13. Ernawan F, Kabir MN (2018) A robust image watermarking technique with an optimal DCT-psychovisual threshold. IEEE Access 6:20464–20480
14. Furqan A, Kumar M (2015, February) Study and analysis of robust DWT-SVD domain based digital image watermarking technique using MATLAB. In: *2015 IEEE international conference on Computational Intelligence & Communication Technology*. IEEE. pp. 638-644
15. Hurrah N, Parah S, Loan N, Sheikh J, Elhoseny M, Muhammad K (2018) Dual watermarking framework for privacy protection and content authentication of multimedia. Futur Gener Comput Syst 94:654–673. https://doi.org/10.1016/j.future.2018.12.036
16. Jane O, Elbasi E, Ilk H (2014) Hybrid non-blind watermarking based on DWT and SVD. J Appl Res Technol 12:750–761
17. Kang XB, Zhao F, Lin GF, Chen YJ (2018) A novel hybrid of DCT and SVD in DWT domain for robust and invisible blind image watermarking with optimal embedding strength. Multimed Tools Appl 77(11): 13197–13224
18. Khare P, Srivastava VK (2018, November) Image watermarking scheme using homomorphic transform in wavelet domain. In: *2018 5th IEEE Uttar Pradesh section international conference on electrical, electronics and computer engineering (UPCON)*. IEEE. pp. 1-6

19. Khare P, Srivastava VK (2018, February) Robust digital image watermarking scheme based on RDWT-DCT-SVD. In: *2018 5th international conference on signal processing and integrated networks (SPIN)*. IEEE. pp. 88-93
20. Khare P, Srivastava VK (2021) A novel dual image watermarking technique using homomorphic transform and DWT. J Intell Syst 30(1):297–311
21. Kumar A (2022) A cloud-based buyer-seller watermarking protocol (CB-BSWP) using semi-trusted third party for copy deterrence and privacy preserving. *Multimed Tools Appl* 81:21417–21448
22. Li J, Yu C, Gupta BB, Ren X (2018) Color image watermarking scheme based on quaternion Hadamard transform and Schur decomposition. Multimed Tools Appl 77(4):4545–4561
23. Liu XL, Lin CC, Yuan SM (2016) Blind dual watermarking for color images' authentication and copyright protection. IEEE Trans Circuits Syst Video Technol 28(5):1047–1055
24. Liu J, Huang J, Luo Y, Cao L, Yang S, Wei D, Zhou R (2019) An optimized image watermarking method based on HD and SVD in DWT domain. IEEE Access 7:80849–80860
25. Nandi S, Santhi V (2016) DWT–SVD-based watermarking scheme using optimization technique. In: Artificial intelligence and evolutionary computations in engineering systems. Springer, New Delhi, pp 69–77
26. Rao VSV, Shekhawat RS, Srivastava VK (2012, March) A reliable digital image watermarking scheme based on SVD and particle swarm optimization. In: *2012 students conference on engineering and systems*. IEEE. pp. 1-6
27. Singh PK (2022) Robust and imperceptible image watermarking technique based on SVD, DCT, BEMD and PSO in wavelet domain. Multimed Tools Appl 81(16):22001–22026
28. Singh D, Singh SK (2017) DWT-SVD and DCT based robust and blind watermarking scheme for copyright protection. Multimed Tools Appl 76(11):13001–13024
29. Sweldens W (1996) The lifting scheme: a custom-design construction of biorthogonal wavelets. Appl Comput Harmon Anal 3(2):186–200
30. Sweldens W (1998) The lifting scheme: a construction of second-generation wavelets. SIAM J Math Anal 29(2):511–546
31. Thakkar FN, Srivastava VK (2017) A blind medical image watermarking: DWT-SVD based robust and secure approach for telemedicine applications. Multimed Tools Appl 76(3):3669–3697
32. Thakkar F, Srivastava VK (2017) A particle swarm optimization and block-SVD-based watermarking for digital images. Turk J Electr Eng Comput Sci 25(4):3273–3288
33. Verma VS, Jha RK, Ojha A (2015) Significant region based robust watermarking scheme in lifting wavelet transform domain. Expert Syst Appl 42(21):8184–8197
34. Wang Z, Sun X, Zhang D (2007, September) A novel watermarking scheme based on PSO algorithm. In: *International conference on life system modeling and simulation*. Springer, Berlin, Heidelberg. pp. 307-314
35. Yang XS (2009, October) Firefly algorithms for multimodal optimization. In: *International symposium on stochastic algorithms*. Springer, Berlin, Heidelberg. pp. 169-178
36. Zear A, Singh AK, Kumar P (2018) Multiple watermarking for healthcare applications. J Intell Syst 27(1): 5–18

Divyanshu Awasthi received his B.Tech in ECE from the University of Allahabad, India, in 2018, M.Tech in Signal Processing from Motilal Nehru National Institute of Technology Allahabad, India, in 2021. Presently, he is a research scholar at Motilal Nehru National Institute of Technology in Allahabad, India. He is working on projects related to Digital Image Watermarking. His interest areas are Digital Image Processing and Signal Processing.

Vinay Kumar Srivastava received the BE degree in Electronics and Telecommunication Engineering from Govt Engineering College Rewa, MP, India, in 1989, the M Tech degree in Communication Engineering from IIT BHU, Varanasi, India, in 1991, and a Ph.D. degree in Electrical Engineering from IIT Kanpur, India in 2001. After spending a brief period in Indian Telephone Industries Limited, Naini, Allahabad, as an Assistant Executive Engineer, he joined Motilal Nehru National Institute of Technology (MNNIT) Allahabad, India, as a Lecturer in 1992, where he became an Assistant Professor in 2001, Associate Professor in 2006 and Professor in 2010. He has about twenty-five years of teaching and research experience. He has supervised several B Tech projects, fifty M Tech Theses, and seven Ph.D. Theses.